

RESEARCH PAPER

Use of gold nanoparticles in MAGIC-f gels to 18 MeV photon enhancement

Hossein Khosravi¹, Karim Ghazikhanlousani¹, Azizollah Rahimi^{1,2*}

¹Department of Radiology, Faculty of Paramedical, Hamadan University of Medical Sciences, Hamadan, Iran

²Department of Medical Physics, Faculty of Medicine, Ahvaz Jundishapur University of Medical Sciences, Ahvaz, Iran

ABSTRACT

Objective(s): Normoxic MAGIC-f polymer gels are established dosimeters used for three dimensional dose quantifications in radiotherapy. Nanoparticles with high atomic number such as gold are novel radiosensitizers used to enhance doses delivered to tumors. The aim of this study was to investigate the effect of gold nanoparticles (GNPs) in enhancing percentage depth doses (PDDs) within the MAGIC-f gel exposed to linear accelerator (linac) high energy photon beams.

Materials and Methods: The MAGIC-f gel was fabricated based on its standard composition with some modifications. The PDDs in tubes containing the gel were calculated by using a common Monte Carlo code (Geant4) followed by experimental verifications. Then, GNPs with an average diameter of 15 nm and a concentration of 0.1 mM were embedded in the gel, poured into falcon tubes and irradiated with 18 MeV beams of an Elekta linac. Finally, similar experimental and Monte Carlo (MC) calculations were made to determine the effect of using GNPs on some dosimetric parameters of interest.

Results: The results of experimental measurements and simulated MC calculations showed a dose enhancement factor (DEF) of 1.12 ± 0.08 and 1.13 ± 0.04 , respectively due to the use of GNPs when exposed to 18 MeV linac energies.

Conclusion: The results indicated that the fabricated MAGIC-f gel could be recommended as a suitable tool for three dimensional dosimetric investigations at high energy radiotherapy procedures wherein GNPs are used.

Keywords: Dose enhancement factor, GNPs, MAGIC-f gel, Monte Carlo method, Radiotherapy

How to cite this article

Khosravi H, Ghazikhanlousani K, Rahimi A. Use of gold nanoparticles in MAGIC-f gels to 18 MeV photon enhancement. *Nanomed J.* 2019; 6(1): 67-73. DOI: 10.22038/nmj.2019.06.009

INTRODUCTION

Nanotechnology is able to improve cellular targeting and enhance the radiosensitization of cancers. Nanoparticles are 100 to 10000 times smaller than human cells, ranging in size from 10 to 200 nm [1]. Nanoparticles smaller than 50 nm could pass through cell membranes and in the case of smaller than 20 nm they could even pass through blood vessels endothelium [2]. By using different surface modifications, nanoparticles could be used as targeted delivery vehicles to carry chemotherapeutic agents or radiosensitizers to malignant cells [3].

Recently, the use of GNPs in the radiotherapy

has been extensively studied experimentally and by Monte Carlo simulations. According to the reported results, radiation dose delivered to tumors increases when GNPs are used during various radiotherapy modalities. However, the mechanism and possible interaction(s) of radiation with GNPs is still a controversial issue. To resolve such controversies, several Monte Carlo simulations have been carried out. These simulations have been applied to nanoparticles with various dimensions ranged from 2 up to 100 nm. In addition, related biological effects have been reported in case of 1.9 nm nanoparticles [4-9]. However, the direct effect of 1.9 nm gold nanoparticles has not been studied on destructing cancer cells in these studies.

So far, researches studying the effect of GNPs

* Corresponding Author Email: azizrahimi91@gmail.com

Note. This manuscript was submitted on October 3, 2018; approved on November 30, 2018

on increasing the dose delivered to cancer tissues have focused mainly on the kilovoltage (KV) and orthovoltage teletherapy X-Rays (or brachytherapy practices with the same range of energies). An energy dependency for the DEF of GNPs [10-12] has been reported in several studies. In addition, the effect of the size of GNPs in association with photon energy on the doses delivered to cancer cells have been studied [13-15]. Results of the above studies have indicated significant enhancement in the doses delivered to cancer cells at the KV energies and proposed GNPs as the best candidate due to its biocompatibility as well as low toxicity. However, not enough investigations are performed on the DEF of GNPs at high MV energies. At higher MV beams (>2MV), the two processes involved in transferring the energy from incident photons to tissues are the Compton scattering and pair production. These processes could produce high energy electrons with different probabilities. The Compton scattering is a photon-atomic electron interaction with a probability proportional to the effective atomic number (Z_{eff}), whereas the pair production occurs primarily by the interaction of photons with the atomic nuclei and is proportional to $Z^{2.4}$ of the irradiated medium [16, 17].

The ionization chambers, TLDs and films can measure the dose at a point or in two dimensions. These dosimeters are not appropriate for determining dose distributions in three-dimensional geometries [18]. But, it is possible to measure directly three dimensional dose distributions as well as the effects of contrast agents or high Z elements such as iodine and GNPs by using suitable polymer gels. Their dose enhancement effects could be directly quantified as contrast agents which may have uniform dispersion within the gel dosimeters [19-20]. Physical measurements prepared in earlier studies [21, 22] have quantified the dose enhancement created by high Z materials such as iodine in normoxic polymer gels. In fact, polymer gel dosimeters are monomers dispersed in a medium. Ionizing radiations exchange these monomers to polymers through a distinguished mechanism [23]. The polymerization degree is dependent on the absorbed dose in gel dosimeters. After polymerization, magnetic properties of the polymers adjoining protons are changed [24]. These changes could be showed by magnetic resonance imaging (MRI). The MRI spin-spin

relaxation rate $R2=1/T2$ is related to the absorbed dose delivered to the gel phantom [25].

One of the advantages of polymer gels is their direct measurement due to the effects of contrast agents such as GNPs. Contrast agents and high Z materials could have uniform dispersion within the gel dosimeter. Therefore, the effects of such materials could be directly quantified [26, 27]. However, experimental measurements of the dose enhancement produced by contrast agents/high Z materials with other types of dosimeters (such as films and ionization chambers) are complicated.

A novel multi-compartments phantom has been developed for radiochromic dosimetry [28]. This phantom has been designed to mimic a tumor surrounded by normal tissues and loaded with GNPs (50 nm in diameter) at a concentration of 0.5 mM. The novel dosimeter is referred to as the Sensitivity Modulated Advanced Radiation Therapy (SMART) dosimeter. Such dosimeters have been irradiated with 100 KV and 6 MV X-ray energies for which a radiation dose enhancement factor of 1.77 and 1.11 have been reported, respectively.

MAGIC-f gel is successfully adopted as a dosimeter to quantify the effects of dose enhancement by GNPs [26]. It has been concluded that this polymer gel could potentially be used for the assessment of dosimetric effects of GNPs in radiation therapy practices. This gel has also been reported as a suitable tool for performing dosimetric investigations when nanoparticles are used in KV radiation therapy. Recently, normoxic type Polyacrylamide gel (nPAG) dosimeters have been established for three dimensional dose quantification in radiotherapy. Furthermore, this gel has been introduced as an appropriate dosimeter for the quantification of dose variation during the irradiation of the target in which GNPs existed [27].

The current study tried to develop a technique for measuring the DEF resulted from the use of GNPs at 18 MV energy by using the MAGIC-f gel +GNPs. Our aim was to determine the feasibility of using the MAGIC-f gel + GNPs as a suitable dosimeter at high MV radiotherapy practices. We tried to determine the DEF in the presence of GNPs with an average diameter of 15 nm, when irradiated with 18 MV energy of a linac by the MAGIC-f dosimetry. Such DEF was also quantified by using a Monte Carlo simulation code (Geant4) for the same clinical situation.

MATERIALS AND METHODS

Gold nanoparticles synthesis

Gold nanoparticles were synthesized by using sodium citrate reduction method [29]. The GNPs were characterized using the dynamic light scattering (DLS) and also transmission electronic microscopy (TEM) measurements, revealing an average diameter of 15 nm (Fig 1 and 2).

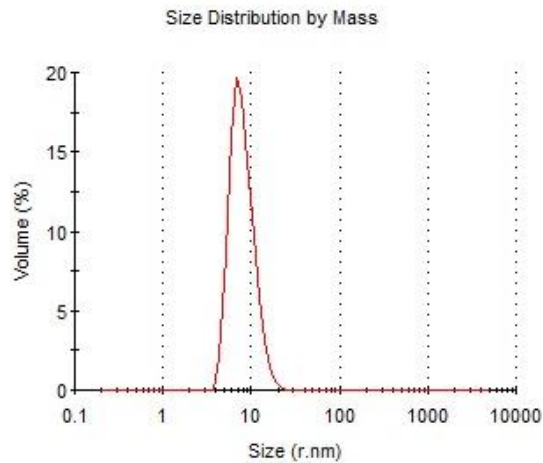


Fig 1. A volumetric size distribution obtained by the DLS measurements for a colloidal sample of the GNPs

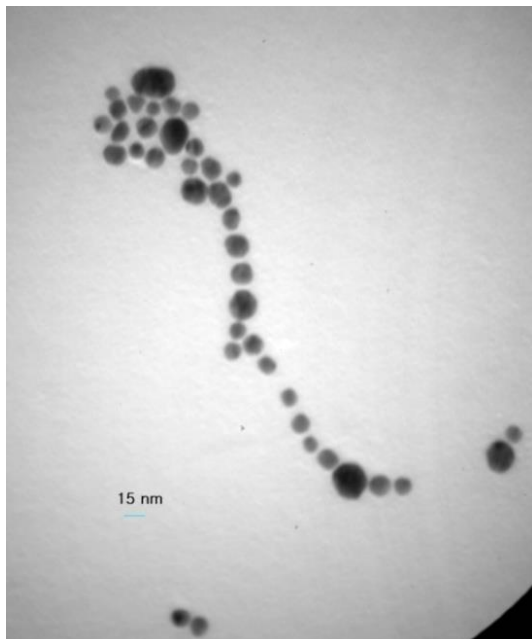


Fig 2. A high resolution Transmission Electron Microscopy image of the synthesized 15 nm GNPs

Gel manufacturing and calibration

The composition used for manufacturing the MAGIC-f gel is presented in Table 1. Such gel

composition results in an effective atomic number of 7.53 and a density of 1.0 g.cm³ making it a tissue equivalent material [30, 31].

Table 1. Composition of the fabricated MAGIC-f gel

Component	Mass concentration (%)
Mili-Q Water	82.31
Gelatin	8.33
Methacrylic acid	5.99
Formaldehyde	3.32
Ascorbic acid	0.03
Copper sulfate	0.02

The final MAGIC-f gel solution was divided into 2 batches. An appropriate concentration of the synthesized GNPs with the average size of 15 nm was added to a specified volume of one of the batches to make a final gel with a GNPs concentration of 0.1 mM (0.0197 mg/ml). The GNPs were added to the mixture in a way to have it embedded homogeneously in the gel. The second batch of the gel (without the GNPs) was used as the control.

The gels were then quickly poured into separate falcon tubes. All samples were placed in the refrigerator (at about 4°C) for 24 hr.

The fabrication of any gel dosimeter, even with the same compositions and conditions, would lead to a unique gel due to inevitable variations such as thermal conditions and constituent concentration occurred during their fabrication. Therefore, every gel dosimeter formulation requires to be calibrated separately during its preparation. Such gel calibration process could affect the accuracy of the fabricated dosimeter. Several factors are recommended for gel dosimeter calibration [32] including i) several tubes, ii) several beams, iii) depth doses and iv) self-consistent normalized methods.

In this study, the method used for gel dosimeter calibration was based on several gel tubes in which several calibration tubes were placed at 10 cm depth of a big container filled with distilled water to provide a uniform medium around them during irradiation. A separate tube was also kept outside as the control while other tubes were irradiated at known levels of 100, 200, 350, 600, and 900 cGy doses provided by the Electra linac. To assure the accuracy and reproducibility of the dosimeter calibration, the above process was repeated three times and their relevant mean values were calculated and used against the dose levels.



Fig 3. The arrangement of the MAGIC-f gel tubes prepared to be irradiated by a linac 18 MV beam

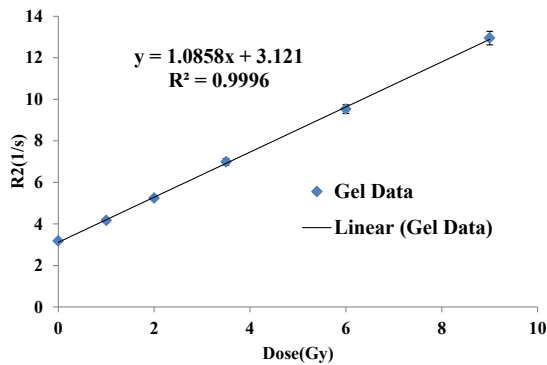


Fig 4. The calibration curve of the MAGIC-f gel drawn from its response to the 18 MeV beams characterized by its R2 MRI signals against the relevant radiation dose levels

Irradiation procedures

Gel samples were irradiated to 18 MeV photon beams of an Electra linac at a 25×25 cm² field size and a SSD of 100 cm. The gel samples (with or without GNPs) were irradiated to different levels of radiation up to 600 cGy (Fig 3). The distance between the water surface of the phantom and the top of the gel samples, along the central axis, was 4 cm.

For calibrating the MAGIC-f gel [25-27], the calibration falcon tubes containing the gel were fixed in a water-filled phantom. The tubes were irradiated to various doses ranged from 0 to 900 cGy. A water equivalent box was positioned under the gel tubes to guarantee a constant backscattering condition.

MRI reading

Dose measurements of the gel samples were

made by relaxometry, which correlates the dose with nuclear magnetic transversal relaxation rate (R2) [33]. Experiments were carried out by using a Siemens 1.5 Tesla MRI scanner 48 h after each irradiation procedure. A multi-spin echo sequence was used with 16 echoes, 22 ms echo time, 3000 ms repetition time, and 0.5×0.5 mm² pixel size. The average of the two acquisitions made for each sample was taken as its reading.

To ensure that the resulting R2 values were not influenced by possible temperature gradients in the gels, the gel samples were kept in the MRI room for a period of 4 hr prior scanning. Each sample was scanned three times to reduce the uncertainties due to the noise in the T2 (spin–spin relaxation time) measurements.

The resulting R2 (=1/T2) maps and their data processing were performed by using the MATLAB software.

Monte Carlo simulations

Computational MC simulations for dose calculations were performed by using the Geant4 code [38]. A water phantom with a dimension of 40×40×30 cm³ was simulated to score dose distributions. Inside the water phantom, the same numbers of cylindrical tubes, as used in experimental stage, were defined. Each simulated tube had the same diameter of 1.4 cm and height of 8 cm as the real ones.

The gold nanospheres with a diameter of 15 nm were uniformly distributed into a nanoparticle region (inside the cylindrical sample) in a grid size of 0.001×0.001×0.001 mm³. Each tally, having a dimension of 2×2×2 mm³, contained 8,000,000,000 gold nanospheres. The total number of all nanospheres in our MC model was 1.96×10¹³ yielding the same concentration of 0.1 mM for the gold nanospheres solution as that of the experimental stage. The used irradiation parameters (SSD, field size, prescribed dose, etc.) in the MC simulations were exactly the same parameters used in the experimental stage. The cross sections determined in Geant4 code for the 18 MeV clinical beams were used for obtaining the similar percentage depth dose curves (PDD) by the MC simulations as those of the experimental measurements.

The cut-off energy for the photons and electrons were set at 0.1 KeV. The number of photon histories for each simulation was set at 4×10⁷ to ensure a statistical uncertainty less than 1% for all the dose scoring cells.

Table 2. The means and standard deviations of the R2 values of MRI images determined from the ROI of every tube irradiated to various known levels of radiation doses

MRI reading	Test no.	Dose (cGy)					
		0 (control)	100	200	350	600	900
R2(1/S)±SD	1	3.21±0.08	4.22±0.17	5.41±0.12	7.11±0.26	9.78±0.34	13.14±0.48
	2	2.91±0.09	3.94±0.11	5.33±0.09	6.89±0.22	9.65±0.32	12.79±0.65
	3	3.42±0.11	4.35±0.15	5.01±0.10	6.97±0.34	9.16±0.43	12.92±0.57
Mean±SD		3.18±0.05	4.17±0.08	5.25±0.06	6.99±0.16	9.53±0.21	12.95±0.33

Statistical analysis

Their percent mean errors were estimated and used as proposed in previous studies to compare various dosimetric parameters obtained from our experimental measurements with those calculated with the MC code [34]. These errors were calculated by using the following formula: Error (%) = 100 × (Simulation Data - Experimental Data) / Experimental Data

RESULTS

The determined relevant R2 values of MRI images for every tube irradiated to various known levels of radiation doses are presented in Table 2. The R2 values calculated from the MRI images of any tube represent the average value of its' relevant ROI (A rectangle with 5 cm length and 1 cm width) along with their standard deviation (SD) values.

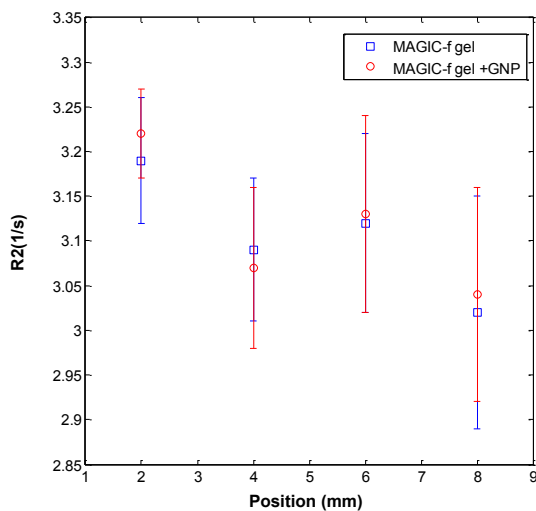


Fig 5. The R2 value measured for unirradiated gel with and without GNPs

Fig 5 shows the calibration curve of the MAGIC-f gel drawn from its response to the linac 18 MeV photon beams characterized by its R2 MRI signals against relevant radiation dose levels. As could be seen in the Figure 4, the gel calibration curve is almost linear (R2=0.9996) within a range of doses from 0 to 900 cGy with a sensitivity about 1.0858 (s.cGy)⁻¹.

The effects of GNPs on polymerization of the unirradiated samples with and without the GNPs were evaluated as shown Fig 5.

The lack of variation difference between the MAGIC-f gel and MAGIC-f gel+GNPs which is less than 1 % indicates that chemical interaction between GNPs and gels are negligible.

Comparison of the PDDs (after the build up region) derived from the MAGIC-f gel response to the 18 MeV photon beams with those calculated by the MC simulations is illustrated in Fig 6.

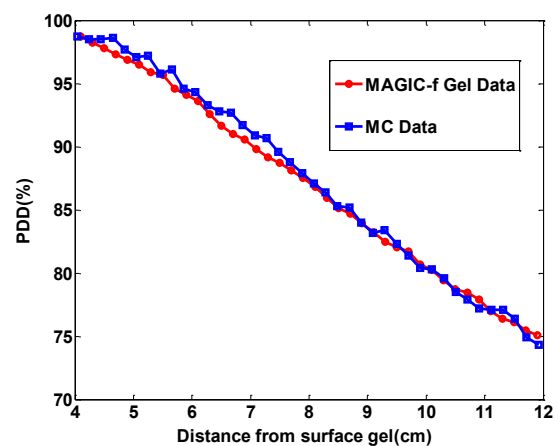


Fig 6. Comparison of the PDDs measured experimentally with the MAGIC-f gel with those calculated by the MC simulations in the gel phantom

Fig 7 shows the measured experimental PDDs in the MAGIC-f gel samples with and without GNPs. As could be seen from the Fig 7, when GNPs (with a concentration of 0.1 mM) are added to the gel dosimeter, the PDDs increased significantly after the buildup region in the gel resulting in a mean DEF of 1.12 ± 0.08 .

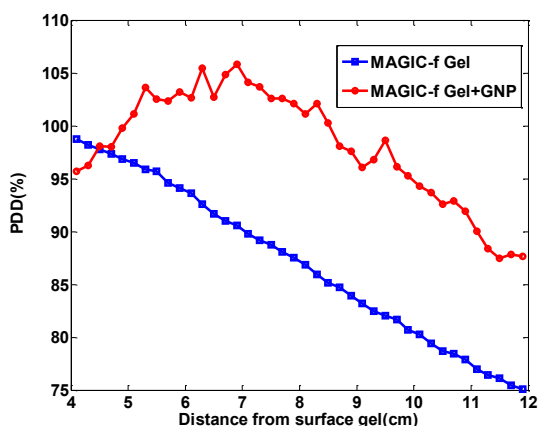


Fig 7. Comparison between the PDDs measured experimentally in the MAGIC-f alone and GNP_MAGIC-f gels

Fig 8 illustrates the calculated PDDs with the MC simulation in the MAGIC-f gel samples with and without GNPs. The MC results shown in this Fig 8 also indicate that when GNPs (with a concentration of 0.1 mM) are considered to be present in the gel, the PDDs increased significantly leading to a mean DEF of 1.13 ± 0.04 .

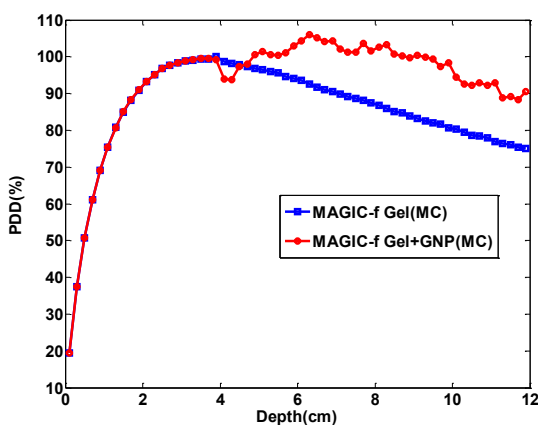


Fig 8. Comparison between the PDDs calculated with the MC simulations in the MAGIC-f alone and GNP_MAGIC-f gels

DISCUSSION

As could be noted more precisely from Fig 8 and 9, there is a small reduction in the PDDs at

a depth located nearly at the corresponding interface of the water and the MAGIC-f gel + GNPs. Thereafter, the DEF follows a slow stable increase. This phenomenon could be attributed to the interface of the two regions (the gels with or without GNPs) which decreased at higher depths where new local charge equilibrium is attained and the pair production interaction with GNPs contributes more in the dose levels.

The mean percentage error derived from the comparison of the MAGIC-f and MAGIC-f gel + GNPs were 0.75% and 1.46% for the calculated MC and measured experimental PDDs, respectively (Fig 9).

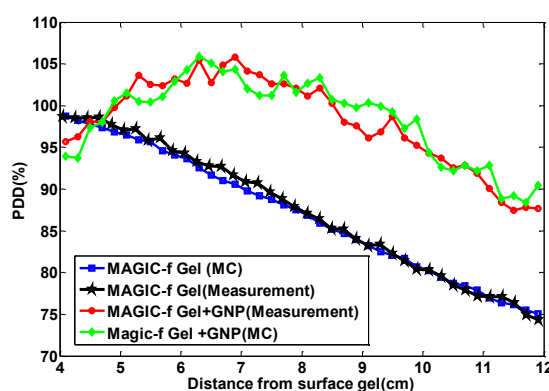


Fig 9. Comparison of the PDDs derived from the calculated MC simulations and experimental measurements in the MAGIC-f gel with and without the GNPs

The DEFs were derived by dividing the doses in the MAGIC-f gel + GNPs to that of the MAGIC-f gel alone derived from either the relevant experimental measurements or MC calculations. The measured doses in the gels are related to the dose indicator factor "T2" taken from the MRI images. The resulting observed DEFs in this study could be attributed to the inclusion of GNPs into the polymer gels as their chemical properties should have been affected eventually and resulted in the enhancement of the absorbed doses.

Our results indicated a significant dose enhancement effect resulted from the use of linac higher photon beams (18 MeV) in the presence of 15 nm GNPs in the MAGIC-f gel dosimeter. The DEFs observed in the presence of high Z materials such as GNPs, as noted in this study, is believed to cause predominant enhancement in the likelihood of the pair production interaction [16-17] resulted from increasing probability of the cross section of this interaction in the presence of GNPs at higher

18 MeV linac energies.

CONCLUSION

The purpose of this study was to develop a technique to measure the DEFs generated by GNPs at higher radiotherapy energies (18 MeV) by using the MAGIC-f gel providing 3D dosimetry. Although previous experimental and MC studies have also confirmed significant DEFs due to adding GNPs to various media [35-37], including the MAGIC-f and other gel dosimeters [26-27], the focus of such studies has mainly been on the KeV energies.

In this work, the fabricated gels were exposed to much higher linac photon energies (18 MeV). In a previous study [17], a DEF of 7% has been reported due to the use of 1.9 nm GNPs when exposed to 6 MeV linac energy only based on the MC dosimetry method and without any experimental measurements validating such results. The difference between our estimated DEF and the above study could be attributed to the different sizes of the GNPs as well as much higher 18 MeV energies, we used.

The main finding of this study was to prove that even at higher 18 MeV energies, a significant DEF (about 12%) can be obtained when 15 nm GNPs are used within a tissue equivalent material (the MAGIC-f gel dosimeter). Our simulated MC calculations also proved this fact by indicating roughly the same amount of DEF (about 13%) due to the presence of GNPs when exposed to 18 MeV linac energy.

Quantification of the dose enhancement due to GNPs using the polymer gels was successfully achieved in this research. However, it must be noted that previous studies have shown that the size and shape of the nanoparticles could influence their intracellular and intratumoral uptake that possibly affects the dose enhancement at KeV energies [13].

Hence, further in vivo investigations are required to examine the findings of this study obtained in the MAIC-f gel media at higher MeV energies.

ACKNOWLEDGMENTS

This study is resulted from a research project carried out by the author at Hamadan University of Medical Sciences with the collaboration of Mahdiyeh Diagnostic and Treatment Center in Hamadan, Iran.

REFERENCES

- 1.Hainfeld JF, Slatkin DN, Smilowitz HM. The use of gold nanoparticles to enhance radiotherapy in mice. *Phys Med Biol.* 2004; 49(18): 309-315.
- 2.Yih TC, Wei C, Hammad B. Modeling and characterization of a nanoliter drug-delivery MEMS micropump with circular bossed membrane. *Nanomedicine.* 2005; 1(2): 164-175.
- 3.Kawasaki ES, Player A. Nanotechnology, nanomedicine, and the development of new, effective therapies for cancer. *Nanomedicine.* 2005; 1(2): 101-109.
- 4.Hirsch L, Stafford R, Serksen N, Halas N, Hazle J, West J. Nanoshell-assisted tumor ablation using near infrared light under magnetic resonance guidance. *Proc Natl Acad Sci.* 2003; 100: 113549-113554.
- 5.Liu Y, Zhang P, Feifei I, Jin X, Li J, Chen W, Li Q. Metal-based NanoEnhancers for Future Radiotherapy: Radiosensitizing and Synergistic Effects on Tumor Cells. *Theranostics.* 2018; 8(7): 1824-1849.
- 6.Loo C, Lowery A, Halas N, West J, Drezek R. Immunotargeted nanoshells for integrated cancer imaging and therapy. *Nano lett.* 2005; 5(4): 709-711.
- 7.Mesbahi A. A review on gold nanoparticles radiosensitization effect in radiation therapy of cancer. *Rep Pract Oncol Radiother.* 2010; 15(6): 176-180.
- 8.Mukherjee P, Bhattacharya R, Bone N, Lee YK, Patra CR, Wang S, Lu L, Secreto C. Potential therapeutic application of gold nanoparticles in B-chronic lymphocytic leukemia (BCLL): enhancing apoptosis. *J Nanobiotechnology.* 2007; 5(1): 4.
- 9.Praetorius NP, Mandal TK. Engineered nanoparticles in cancer therapy. *Recent Pat Drug Deliv Formul.* 2007; 1(1): 37-51.
- 10.Cho J, Gonzalez-Lepera C, Manohar N, Kerr M, Krishnan S, Cho SH. Quantitative investigation of physical factors contributing to gold nanoparticle-mediated proton dose enhancement. *Phys Med Biol.* 2016;61(6):2562-2581.
- 11.Geng F, Xing JZ, Chen J, Yang R, Hao Y, Song K, Kong B. Pegylated glucose gold nanoparticles for improved in-vivo bio-distribution and enhanced radiotherapy on cervical cancer. *J Biomed Nanotechnol.* 2014;10(7):1205-1216.
- 12.Taggart LE, McMahan SJ, Currell FJ, Prise KM, Butterworth KT. The role of mitochondrial function in gold nanoparticle mediated radiosensitisation. *Cancer Nanotechnol.* 2014; 5(1): 5.
- 13.Chithrani BD, Ghazani AA, Chan WC. Determining the size and shape dependence of gold nanoparticle uptake into mammalian cells. *Nano lett.* 2006; 6(4): 662-668.
- 14.Leung MK, Chow JC, Chithrani BD, Lee MJ, Oms B, Jaffray DA. Irradiation of gold nanoparticles by x-rays: Monte Carlo simulation of dose enhancements and the spatial properties of the secondary electrons production. *Med phys.* 2011; 38(2): 624-631.
- 15.Zhang SX, Gao J, Buchholz TA, Wang Z, Salehpour MR, Drezek RA. Quantifying tumor-selective radiation dose enhancements using gold nanoparticles: a monte carlo simulation study. *Biomed Microdevices.*

- 2009; 11(4): 925-933.
16. Alkhatib A, Watanabe Y, Broadhurst JH. The local enhancement of radiation dose from photons of MeV energies obtained by introducing materials of high atomic number into the treatment region. *Med phys.* 2009; 36(8): 3543-3548.
 17. Kirkby C, Ghasroddashti E. Targeting mitochondria in cancer cells using gold nanoparticle-enhanced radiotherapy: A Monte Carlo study. *Med phys.* 2015; 42(2): 1119-1128.
 18. Khan FM, Gibbons JP. Khan's the physics of radiation therapy: Lippincott Williams & Wilkins; 2014.
 19. Morris KN, Weil MD, Malzbender R. Radiochromic film dosimetry of contrast-enhanced radiotherapy (CERT). *Phys Med Biol.* 2006; 51(22): 5915-2925.
 20. Robar JL, Riccio SA, Martin M. Tumour dose enhancement using modified megavoltage photon beams and contrast media. *Phys Med Biol.* 2002; 47(14): 2433-2449.
 21. Boudou C, Troprès I, Rousseau J, Lamalle L, Adam J-F, Estève F. Polymer gel dosimetry for synchrotron stereotactic radiotherapy and iodine dose-enhancement measurements. *Phys Med Biol.* 2007; 52(16): 4881-4892.
 22. Gastaldo J, Boudou C, Lamalle L, Troprès I, Corde S, Sollier A. Normoxic polyacrylamide gel doped with iodine: response versus X-ray energy. *Eur J Radiol.* 2008; 68(3): S118-S120.
 23. Abtahi S. Characteristics of a novel polymer gel dosimeter formula for MRI scanning: dosimetry, toxicity and temporal stability of response. *Phys Med.* 2016; 32(9): 1156-1161.
 24. Lee HJ, Roed Y, Venkataraman S, Carroll M, Ibbott GS. Investigation of magnetic field effects on the dose-response of 3D dosimeters for magnetic resonance-image guided radiation therapy applications. *Radiother Oncol.* 2017; 125(3): 426-432.
 25. De Deene Y, De Wagter C, De Neve W, Achten E. Artefacts in multi-echo T2 imaging for high-precision gel dosimetry: I. Analysis and compensation of eddy currents. *Phys Med Biol.* 2000; 45(7): 1807-1823.
 26. Marques T, Schwarcke M, Garrido C, Zucolot V, Baffa O, Nicolucci P, editors. *Gel dosimetry analysis of gold nanoparticle application in kilovoltage radiation therapy. JPCS*; 2010: IOP Publishing.
 27. Rahman WN, Wong CJ, Ackerly T, Yagi N, Geso M. Polymer gels impregnated with gold nanoparticles implemented for measurements of radiation dose enhancement in synchrotron and conventional radiotherapy type beams. *Australas Phys Eng Sci Med.* 2012; 35(3): 301-309.
 28. Alqathami M, Blencowe A, Yeo UJ, Doran SJ, Qiao G, Geso M. Novel multicompart ment 3-dimensional radiochromic radiation dosimeters for nanoparticle-enhanced radiation therapy dosimetry. *Int J Radiat Oncol Biol Phys.* 2012; 84(4): e549-e555.
 29. Sobczak-Kupiec A, Malina D, Zimowska M, Wzorek Z. Characterization of gold nanoparticles for various medical application. *Dig J Nanomater Biostruct.* 2011; 6(2): 803-808.
 30. Fernandes JP, Pastorello BF, de Araujo DB, Baffa O. Formaldehyde increases MAGIC gel dosimeter melting point and sensitivity. *Phys Med Biol.* 2008; 53(4): N53-58.
 31. Pavoni J, Pike T, Snow J, DeWerd L, Baffa O. Tomotherapy dose distribution verification using MAGIC-f polymer gel dosimetry. *Med phys.* 2012; 39(5): 2877-2884.
 32. McJury M, Oldham M, Cosgrove V, Murphy P, Doran S, Leach M. Radiation dosimetry using polymer gels: methods and applications. *Br J Radiol.* 2000; 73(873): 919-929.
 33. De Deene Y, Van de Walle R, Achten E, De Wagter C. Mathematical analysis and experimental investigation of noise in quantitative magnetic resonance imaging applied in polymer gel dosimetry. *Sig Process.* 1998; 70(2): 85-101.
 34. Sheikh-Bagheri D, Rogers D, Ross CK, Seuntjens JP. Comparison of measured and Monte Carlo calculated dose distributions from the NRC linac. *Med phys.* 2000; 27(10): 2256-2266.
 35. Khosravi H, Hashemi B, Mahdavi S, Hejazi P. Effect of gold nanoparticles on prostate dose distribution under Ir-192 internal and 18 MV external radiotherapy procedures using gel dosimetry and monte carlo method. *J Biomed Phys Eng.* 2015; 5(1): 3-14.
 36. McNamara A, Kam W, Scales N, McMahon S, Bennett J, Byrne H. Dose enhancement effects to the nucleus and mitochondria from gold nanoparticles in the cytosol. *Phys Med Biol.* 2016; 61(16): 5993-6010.
 37. Rehman MU, Jawaid P, Kondo T. *Dual Effects of Nanoparticles on Radiation Therapy: as Radiosensitizers and Radioprotectors. REM.* 2016; 5: 40-45.
 38. <https://geant4.web.cern.ch>.